

## Supporting Information

### Accelerated discovery of defect tolerant organo-halide perovskites

N. Isleyen, A. Corcor, S. Cakirefe, N. Ormanlı, E. N. Kanat, and I. Yavuz\*

Department of Physics, Marmara University, 34722, Ziverbey, Istanbul, Turkey.

#### AUTHOR INFORMATION

##### \*Corresponding Author

e-mail: [ilhan.yavuz@marmara.edu.tr](mailto:ilhan.yavuz@marmara.edu.tr)

### Note S1. Chemical potential calculations:

For the calculation of chemical potentials  $\mu_A$ ,  $\mu_B$ ,  $\mu_X$  forming the  $ABX_3$  perovskite, we will follow the procedure by Yin et. al and others [S1-S4]. In this approach, we first assume that  $ABX_3$  perovskite phase and some secondary phases (vide infra) are in their thermodynamic equilibrium such that  $\mu_A < 0$ ,  $\mu_B < 0$  and  $\mu_X < 0$ . Therefore, we can write

$$\mu_A + \mu_B + 3\mu_X = \Delta H_f(ABX_3) \quad (\text{S1})$$

thermodynamic condition for the formation of  $ABX_3$ . Here,  $\Delta H_f(ABX_3)$  is the orthorombic phase formation energy of  $ABX_3$ . We calculate the formation energy of  $ABX_3$  using  $\Delta H_f(ABX_3) = H(ABX_3) - [H(A) + H(B) + 3H(X)]$ , where  $H(ABX_3)$ ,  $H(A)$ ,  $H(B)$ ,  $H(X)$  are separately the energies of  $ABX_3$ , A, B, and X crystals, respectively. In addition the following constraints must also be satisfied in order avoid the formation of secondary phases

$$\mu_A + \mu_X < \Delta H_f(AX) \quad (\text{S2})$$

$$\mu_B + 2\mu_X < \Delta H_f(BX_2) \quad (\text{S3})$$

Here  $\Delta H_f(AX)$  and  $\Delta H_f(BX_2)$  are the formation energies of the  $AX$  and  $BX_2$  phases found from  $\Delta H_f(AX) = H(AX) - [H(A) + H(X)]$  and  $\Delta H_f(BX_2) = H(BX_2) - [H(B) + 2H(X)]$ . These S1 - S3 conditions enable the selection window in chemical potential space, which is shown by diagrams in **Diagram S1**.

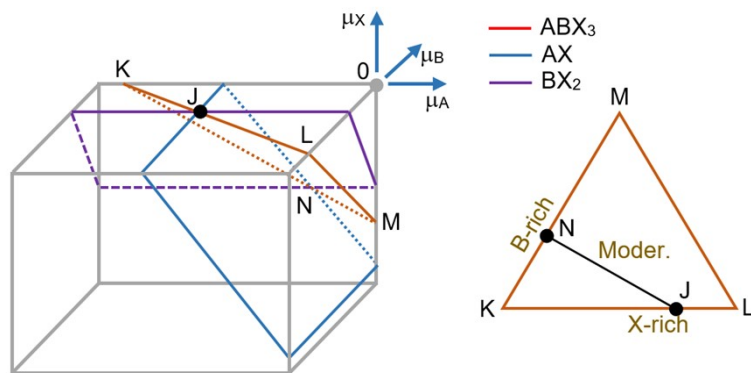


**Diagram S1.** (left) Chemical-potential space with axes  $\mu_A$ ,  $\mu_B$  and  $\mu_X$  and the region in space satisfies the restrictions in Eq. S1-S3. Each planes represent the region of  $ABX_3$ ,  $AX$  and  $BX_2$  formations. (right) A triangular diagram extracted from the left diagram showing the points of B-rich, X-rich and moderate conditions.

First of all, for the DFT calculations of  $H(A)$  of 32 different A-sites in **Diagram S2**, simple cubic phase is considered. For  $H(B)$  of 36 different B-sites (here 36 of 43 are in the 2700 HOIP candidates), cubic phase is considered. The unit-cell crystal structures of the X-site ( $X = \text{Cl}, \text{F}, \text{Br}$  and I) shown in **Figure S1** are used for the DFT calculations of  $H(X)$ . Within our randomly selected 240  $ABX_3$  HOIP structures for DFT calculations out of 2700 HOIP candidates, we saw that there appears to be 92 unique B-X and 101 unique A-X site pairs (*e.g.*,  $\text{MAPbI}_3$  and  $\text{FAPbI}_3$  have different A-X pair but the same B-X pair). For the DFT calculations of 92 unique  $H(AX)$ , cubic phase is considered. For  $H(BX_2)$ , however, we first used trigonal phase for all 101 unique structures. But we then observed 14 of the 101  $BX_2$  structures,  $\Delta H_f(BX_2) > 0$  such that  $BX_2$  trigonal phase for them is predicted to be unstable. We then payed special attention to those 14 structures and obtained their appropriate crystal structures and stoichiometries (as  $BX$ ,  $BX_3$  and  $BX_4$ ) based on the formation energies with the help of Materials Project Database (<https://materialsproject.org/>) .

### Note S2. Finite-size correction calculations:

$E_{corr}$ , finite-site energy correction calculations of 240  $V_X$  and 240  $X_i$  HOIP defects for different charge-states are performed based on the Freysoldt–Neugebauer–van de Walle (FNV) scheme [S5-S7]

$$E_{corr} = E_q^{latt} - q[V_{0/p} + V_{q/0-m}] \quad (\text{S4})$$

The correction includes; lattice correction  $E_q^{latt}$  and potential alignments  $V_{q/0-m}$  and  $V_{0/p}$ , which are expressed below,

$$E_q^{latt} = E_q^{iso,m} - E_q^{per,m} \quad (\text{S5})$$

$$V_{0/p} = V_0|_{far} - V_p \quad (\text{S6})$$

$$V_{q/0-m} = [V_q - V_0]_{far} - V_q^{per,m}|_{far}, \quad (\text{S7})$$

where  $E_q^{iso,m}$  and  $E_q^{per,m}$  model energies of the isolated defect and periodic defect at the q-state, respectively.  $V_0|_{far}$  is the potential of the neutral defect far from location of the defect and  $V_p$  is the potential of the pristine host material.  $[V_q - V_0]_{far}$  is the DFT calculated potential difference between the charged and neutral defect far from the location of the defect and  $V_q^{per,m}|_{far}$  is the

model potential value of the periodic one far from the defect.

The calculation of Eq. S5 requires the calculation of relative permittivity of each 240 HOIP structures that we considered from the ML training. For this, we used a simplified model; we used

the Clausius–Mosotti relation  $\epsilon_r = 1 + \frac{12\pi\alpha n}{3 - 4\pi\alpha n}$ , where  $\alpha$  is the polarizability and  $n = N/V$ ,  $N$  is the number of particles and  $V$  is the cell volume. We used the atomic polarizabilities for B and X site and molecular polarizabilities which we calculated from the GAMESS package [S8]. We checked and saw that the average  $\epsilon_r$  (calculated over the 240 HOIP structures) is  $\sim 7.52$ , which is a reasonable value for HOIPs. Lattice energy correction calculations are performed using COEFFE python software [S9].

Since we are interested in the vacancy and interstitial halide defect  $V_X$  and  $X_i$ , chemical potentials of  $\mu_X$  are only reported for different growth conditions (X-rich:  $\mu_X = 0$ , B-rich:  $\mu_B = 0$  and moderate). The distribution of  $\mu_X$  chemical potentials are shown in **Figure S2**.

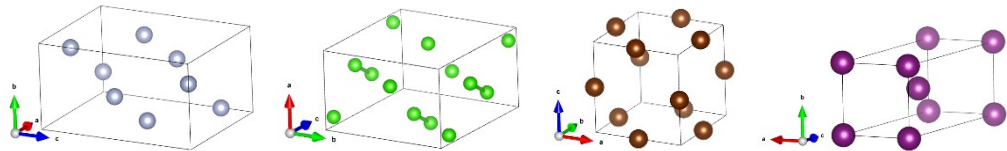
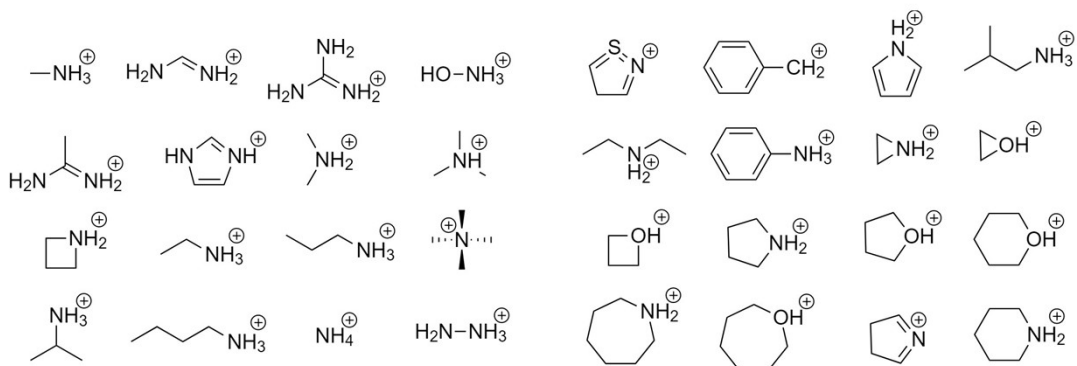


**Figure S1.** Unit cell structures of Cl, F, Br, I crystals we considered in chemical potential calculations.



A01	[CH <sub>3</sub> NH <sub>3</sub> ]	A12	[(CH <sub>3</sub> ) <sub>4</sub> N]	A23	[C <sub>2</sub> NH <sub>6</sub> ]
A02	[CH(NH <sub>2</sub> ) <sub>2</sub> ]	A13	[(CH <sub>3</sub> ) <sub>2</sub> CHNH <sub>3</sub> ]	A24	[C <sub>2</sub> OH <sub>5</sub> ]
A03	[(NH <sub>2</sub> ) <sub>3</sub> C]	A14	[CH <sub>3</sub> (CH <sub>2</sub> ) <sub>3</sub> NH <sub>3</sub> ]	A25	[C <sub>3</sub> OH <sub>7</sub> ]
A04	[NH <sub>3</sub> OH]	A15	[NH <sub>3</sub> ] <sub>2</sub>	A26	[C <sub>4</sub> NH <sub>10</sub> ]
A05	[CH <sub>3</sub> C(NH <sub>2</sub> ) <sub>2</sub> ]	A16	[NH <sub>3</sub> NH <sub>2</sub> ] <sub>2</sub>	A27	[C <sub>4</sub> OH <sub>6</sub> ]
A06	[C <sub>3</sub> N <sub>2</sub> H <sub>5</sub> ]	A17	[C <sub>3</sub> H <sub>4</sub> NS]	A28	[C <sub>5</sub> OH <sub>12</sub> ]
A07	[(CH <sub>3</sub> ) <sub>2</sub> NH <sub>2</sub> ]	A18	[C <sub>7</sub> H <sub>7</sub> ]	A29	[C <sub>6</sub> NH <sub>14</sub> ]
A08	[(CH <sub>3</sub> ) <sub>3</sub> NH]	A19	[(CH) <sub>4</sub> NH <sub>2</sub> ]	A30	[C <sub>6</sub> OH <sub>13</sub> ]
A09	[(CH <sub>2</sub> ) <sub>3</sub> NH <sub>2</sub> ]	A20	[C(CH <sub>3</sub> ) <sub>2</sub> CH <sub>2</sub> NH <sub>2</sub> ]	A31	[NC <sub>4</sub> H <sub>8</sub> ]
A10	[(CH <sub>3</sub> CH <sub>2</sub> )NH <sub>3</sub> ]	A21	[(CH <sub>3</sub> ) <sub>2</sub> (CH <sub>2</sub> ) <sub>2</sub> NH <sub>2</sub> ]	A32	[C <sub>5</sub> NH <sub>12</sub> ]
A11	[CH <sub>3</sub> (CH <sub>2</sub> ) <sub>2</sub> NH <sub>3</sub> ]	A22	[C(CH) <sub>5</sub> NH <sub>3</sub> ]		

**Table S1.** Chemical structures of 32 organic cations (as A-site) we considered. **Table:** Short names of A-sites (as An, where n = 01, 02, 03, ..., 32) and their chemical formulas.

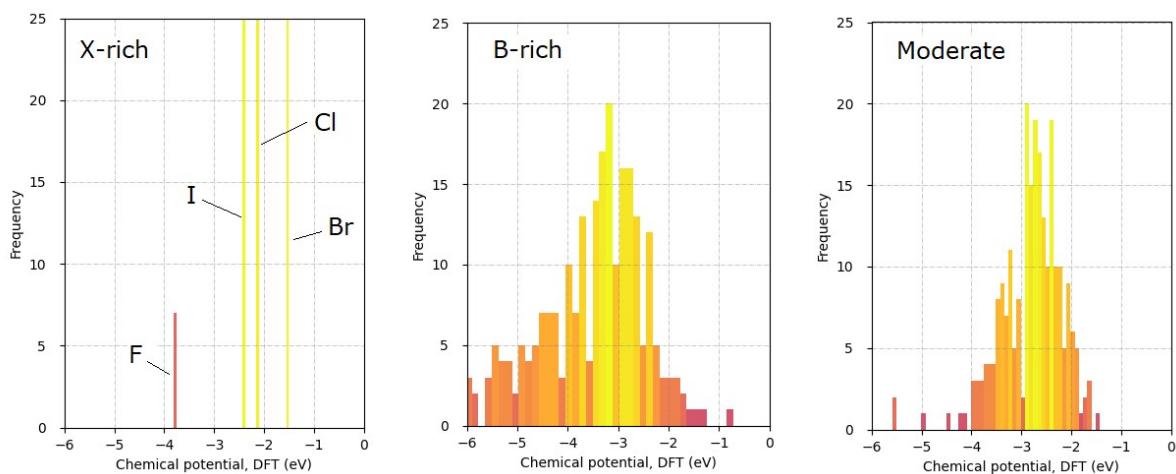


**Figure S2.** DFT calculated chemical-potential distributions,  $\mu_X$ , of 240 HOIP materials for different growth conditions.

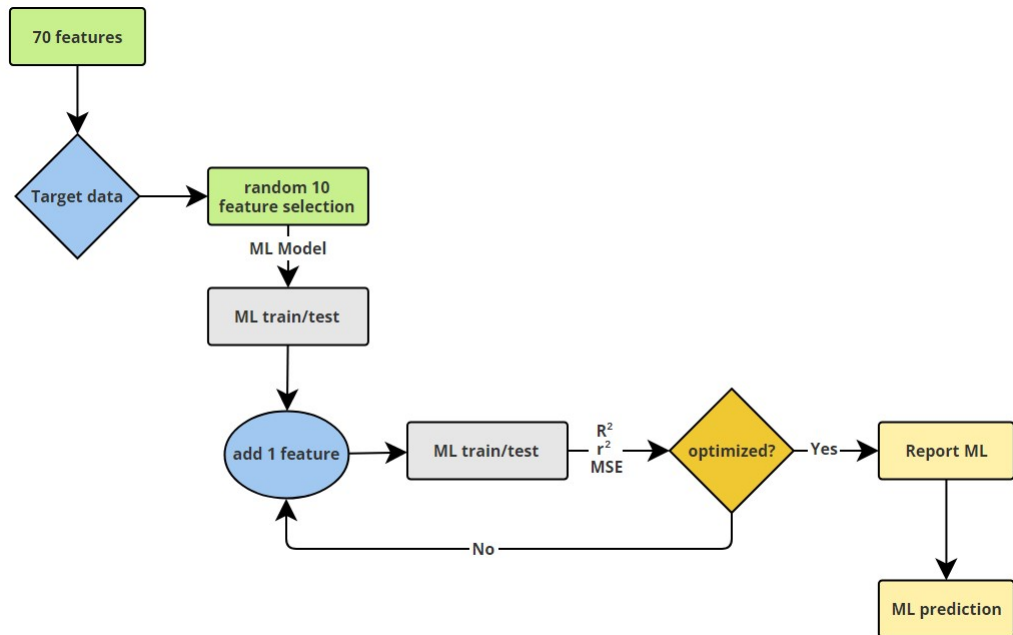


**Chart S1.** Flowchart of our ML procedure to achieve maximum performance with minimum feature selection.

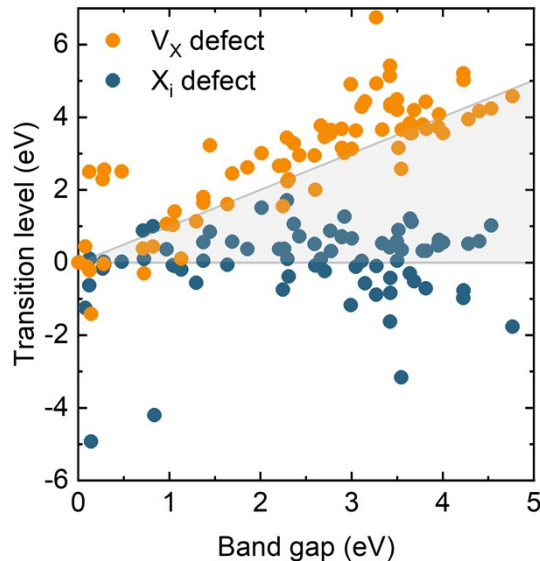


**Figure S3.** DFT calculated transition-levels of  $V_X$  ( $\varepsilon(0/+)$ ) and  $X_i$  ( $\varepsilon(0/-)$ ) defect calculated vs. bandgap of each of the 240 randomly selected HOIP material.

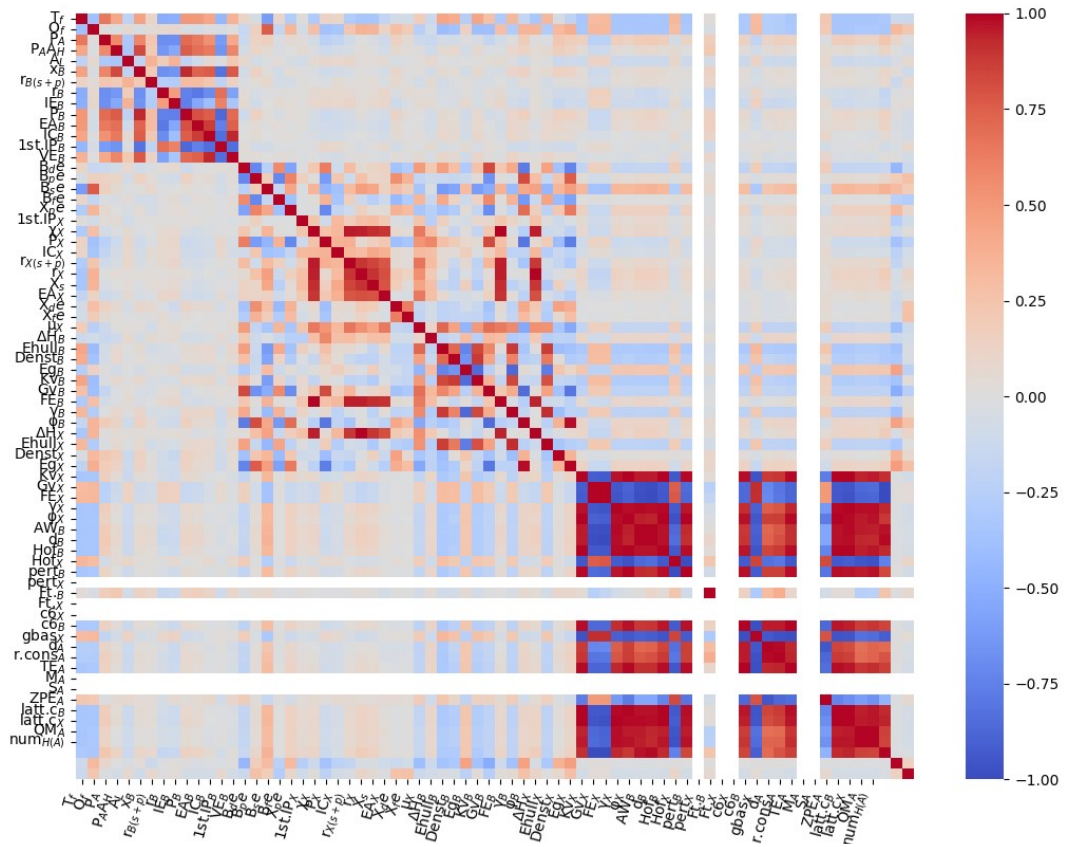


**Figure S4.** Heat-map of Pearson correlation matrix of 70 features we considered.

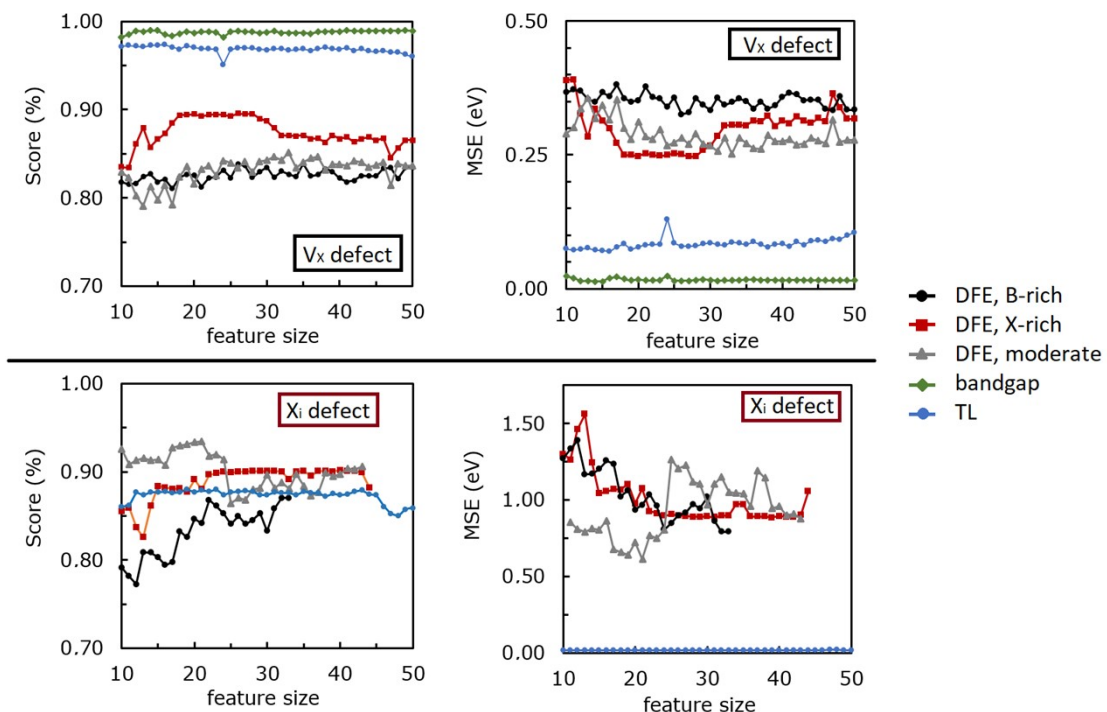


**Figure S5.** Learning performance of GBR algorithm for band gaps, different defects and different growth conditions and transition-levels.

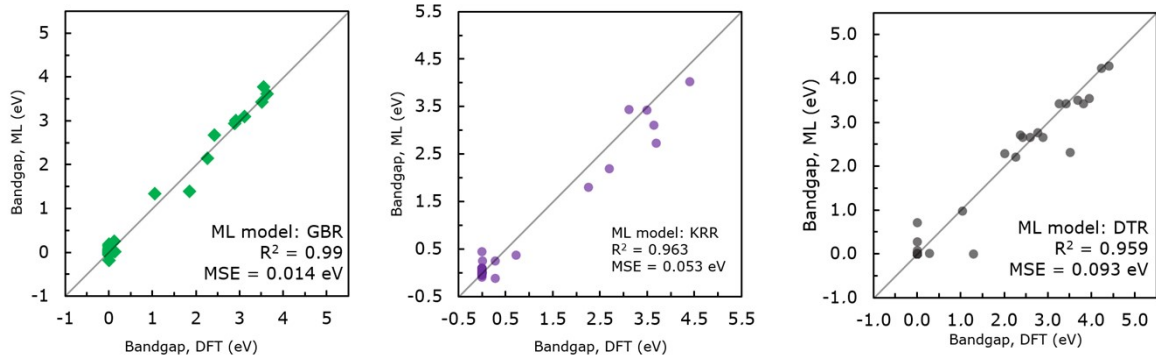


**Figure S6.** Bandgap learning performance of GBR, KRR and DTR algorithms for the test set. DFT calculated bandgap vs. ML prediction. Learning scores and MSEs are given on each figure.

**Table S2.** GBR parameters and scores

		Number of estimators	Loss function	Test size	Score
V <sub>x</sub> defect	Bandgap	100	Huber	0.2	0.99
	CFE	148	Huber	0.08	0.98
	DFE, B-rich	108	Huber	0.08	0.84
	DFE, X-rich	98	Huber	0.08	0.89
	DFE, moderate	98	Huber	0.08	0.85
X <sub>i</sub> defect	TL	98	Huber	0.14	0.97
	DFE, B-rich	162	Huber	0.08	0.93
	DFE, X-rich	114	Huber	0.08	0.90
	DFE, moderate	162	Huber	0.08	0.91
	TL	101	Huber	0.14	0.88

**Table S3.** KRR parameters and scores

		Number of estimator s	Alpha	Degree	Gamma	Kernel	Test size	Score
V <sub>x</sub> defect	Bandgap						0.20	0.96
	CFE		0.10	2	4.0	Poly	0.08	0.97
	DFE, B-rich	98	0.18	2	5.0	Linear	0.08	0.83
	DFE, X-rich	98	0.18	2	5.0	Linear	0.08	0.81
	DFE, mod.	98	0.18	2	5.0	Linear	0.08	0.81
X <sub>i</sub> defect	TL	98	0.18	2	5.0	Poly	0.14	0.95
	DFE, B-rich	114	0.18	2	5.2	RBF	0.08	0.75
	DFE, X-rich	114	0.18	2	5.0	RBF	0.08	0.64
	DFE, mod.	114	0.18	2	7.4	RBF	0.08	0.68
	TL	98	0.18	2	5.0	Sigmoid	0.14	0.83

**Table S4.** DTR parameters and scores

		Criterion	Max features	Splitter	Test size	Score
	Bandgap				0.20	0.96
	CFE	MAE	Auto	Random	0.08	0.95
V <sub>x</sub> defect	DFE, B-rich	MAE	Auto	Best	0.08	0.67
	DFE, X-rich	MSE	Auto	Best	0.08	0.75
	DFE, mod.	MAE	Sqrt	Best	0.08	0.75
	TL	Friedman MSE	Sqrt	Best	0.14	0.98
X <sub>i</sub> defect	DFE, B-rich	Friedman MSE	Sqrt	Best	0.08	0.78
	DFE, X-rich	MAE	Sqrt	Best	0.08	0.81
	DFE, mod.	Friedman MSE	Auto	Best	0.08	0.83
	TL	Friedman MSE	Sqrt	Best	0.14	0.80

CFE: crystal formation energy, DFE: defect formation energy.

**Table S5.** 70 Features, their descriptions and data resource references. <sup>a</sup>Ref. S10 <sup>b</sup> Extracted from Materials Project database using python modules. <sup>c</sup>Ref. S11. Our work: extracted from our DFT calculations using the GAMESS package, except  $\mu_x$  and  $\text{num}_{H(A)}$ .

Features	Descriptions	Resource
$T_f$	Tolerance factor	a
$O_f$	Octahedral factor	a
$r_{A,eff}, r_B, r_X$	Iron radii for the A, B and X site atoms	a
$P_A, P_B, P_X$	Ionic polarizability for the A, B and X site ionic	a
$A_H, A_L$	HOMO and LUMO for the A-site molecules	Our Work
$X_B, X_X$	Martynov-Batsanov electronegativity scales	a
$r_{B(s+p)}, r_{X(s+p)}$	Sum of the s and p orbital radii	a
$IE_B$	Ionization energy for the B site cations	a
$EA_B, EA_X$	Electron affinity for the B site atoms	a
$IC_B, IC_X$	Ionic charge for B and X site cations	a
$1st.IP_B, 1st.IP_X$	The first ionization energy for B and X site atoms	a
$VE_B$	Valence electrons for the B site atoms	a
$\mu_X$	Chemical potential for X site atoms	Our Work
$\Delta H_B, \Delta H_X$	Formation energy for the X and B sites	Materials Project <sup>b</sup>
$E_{hull,B}, E_{hull,X}$	Electron above hull for the X and B sites	Materials Project <sup>b</sup>
$\rho_B, \rho_X$	Density values for the X and B sites	Materials Project <sup>b</sup>
$E_{g,B}, E_{g,X}$	Bandgap for X and B sites	Materials Project <sup>b</sup>
$Kv_B, Kv_X$	Bulk modulus for X and B sites	Materials Project <sup>b</sup>
$Gv_B, Gv_X$	Shear modulus for X and B sites	Materials Project <sup>b</sup>
$E_B, E_X$	Final energy for X and B sites	Materials Project <sup>b</sup>
$\gamma_B, \gamma_X$	Surface energy for the X and B sites	Materials Project <sup>b</sup>
$\Phi_B, \Phi_X$	Work functions for the X and B sites	Materials Project <sup>b</sup>
$M_B$	Atomic mass for B site atoms	Mendeleev <sup>c</sup>
$d_B, d_A$	Dipole polarizability for the A and B sites	Mendeleev <sup>c</sup>
$H_{of,B}, H_{of,X}$	Heat of formation energys for the X and B sites	Mendeleev <sup>c</sup>
$pert_B, pert_X$	Period in periodic table for the B and X sites	Mendeleev <sup>c</sup>
$Ft_B, Ft_X$	Fusion temperature for the X and B sites	Mendeleev <sup>c</sup>
$C_{6,X}, C_{6,B}$	$C_6$ dispersion coefficients for the X and B sites	Mendeleev <sup>c</sup>
$gbas_X$	Gas basicity for the X sites	Mendeleev <sup>c</sup>
$R_A$	Rotational constant for the A sites	Our Work
$E_A$	Total energy of the A site molecules	Our Work
$M_A$	Molar mass of A the site molecules	Our Work
$S_A$	Entropy values of the A site molecules	Our Work
$ZPE_A$	Zero-point energy of the A sites	Our Work
$c_B, c_X$	Lattice constants for the X and B sites	Mendeleev <sup>c</sup>
$Q_A$	Nuclear electric quadrupole moment for the A sites	Our Work
$num_{H(A)}$	Hydrogen number for the A sites	Our Work

**Table S6.** List of 240 candidates randomly selected for ML training from 2700 HOIPs.

A01BiCl <sub>3</sub>	A04BiCl <sub>3</sub>	A07PbBr <sub>3</sub>	A10YbBr <sub>3</sub>	A13WCl <sub>3</sub>	A16RhCl <sub>3</sub>	A20SmCl <sub>3</sub>	A24CoF <sub>3</sub>	A26RhBr <sub>3</sub>	A29PbBr <sub>3</sub>
A01EuCl <sub>3</sub>	A04EuCl <sub>3</sub>	A07PbI <sub>3</sub>	A10ZrCl <sub>3</sub>	A13ZnCl <sub>3</sub>	A16SbBr <sub>3</sub>	A20SrI <sub>3</sub>	A24HgBr <sub>3</sub>	A26SnBr <sub>3</sub>	A29SmCl <sub>3</sub>
A01HgI <sub>3</sub>	A04SbBr <sub>3</sub>	A07PdBr <sub>3</sub>	A11BaI <sub>3</sub>	A14BaBr <sub>3</sub>	A16ScI <sub>3</sub>	A21InI <sub>3</sub>	A24MnBr <sub>3</sub>	A26SnCl <sub>3</sub>	A29SmI <sub>3</sub>
A01PbCl <sub>3</sub>	A04TaI <sub>3</sub>	A07ScI <sub>3</sub>	A11CdI <sub>3</sub>	A14BiCl <sub>3</sub>	A16SrBr <sub>3</sub>	A21MnBr <sub>3</sub>	A24MoBr <sub>3</sub>	A26TiBr <sub>3</sub>	A29SnCl <sub>3</sub>
A01PdCl <sub>3</sub>	A04TII <sub>3</sub>	A07SmBr <sub>3</sub>	A11HgCl <sub>3</sub>	A14CdI <sub>3</sub>	A16TaBr <sub>3</sub>	A21NbCl <sub>3</sub>	A24MoCl <sub>3</sub>	A26TII <sub>3</sub>	A29YbCl <sub>3</sub>
A01PtCl <sub>3</sub>	A04TmBr <sub>3</sub>	A07SrCl <sub>3</sub>	A11MoCl <sub>3</sub>	A14CuCl <sub>3</sub>	A16WCl <sub>3</sub>	A21ScCl <sub>3</sub>	A24SnI <sub>3</sub>	A27EuCl <sub>3</sub>	A29YCl <sub>3</sub>
A01SnI <sub>3</sub>	A05BiI <sub>3</sub>	A07TiCl <sub>3</sub>	A11PbBr <sub>3</sub>	A14MoCl <sub>3</sub>	A16YbI <sub>3</sub>	A21TiBr <sub>3</sub>	A24VCl <sub>3</sub>	A27MnBr <sub>3</sub>	A29ZrI <sub>3</sub>
A01SrI <sub>3</sub>	A05HfI <sub>3</sub>	A07YbCl <sub>3</sub>	A11PbCl <sub>3</sub>	A14ReF <sub>3</sub>	A17BiBr <sub>3</sub>	A21ZrBr <sub>3</sub>	A24YbBr <sub>3</sub>	A27RhBr <sub>3</sub>	A30AgI <sub>3</sub>
A01TiF <sub>3</sub>	A05HgBr <sub>3</sub>	A08HfI <sub>3</sub>	A11PdCl <sub>3</sub>	A14TmI <sub>3</sub>	A17CaI <sub>3</sub>	A22CaBr <sub>3</sub>	A24YbI <sub>3</sub>	A27SbI <sub>3</sub>	A30BiI <sub>3</sub>
A02BiI <sub>3</sub>	A05RhCl <sub>3</sub>	A08HgI <sub>3</sub>	A11SbI <sub>3</sub>	A14VBr <sub>3</sub>	A17SmI <sub>3</sub>	A22CdI <sub>3</sub>	A24YBr <sub>3</sub>	A27WI <sub>3</sub>	A30EuBr <sub>3</sub>
A02MoBr <sub>3</sub>	A05ScBr <sub>3</sub>	A08MoI <sub>3</sub>	A11TmCl <sub>3</sub>	A14WCl <sub>3</sub>	A17SnBr <sub>3</sub>	A22EuI <sub>3</sub>	A24ZnCl <sub>3</sub>	A27YbBr <sub>3</sub>	A30SrI <sub>3</sub>
A02ScI <sub>3</sub>	A05YI <sub>3</sub>	A08PbBr <sub>3</sub>	A11WF <sub>3</sub>	A14YbCl <sub>3</sub>	A17YI <sub>3</sub>	A22MoI <sub>3</sub>	A25BaBr <sub>3</sub>	A28AuBr <sub>3</sub>	A30TaCl <sub>3</sub>

A02SrBr <sub>3</sub>	A06AuCl <sub>3</sub>	A08PdBr <sub>3</sub>	A11YBr <sub>3</sub>	A14ZrBr <sub>3</sub>	A18SrI <sub>3</sub>	A22SrBr <sub>3</sub>	A25BiCl <sub>3</sub>	A28BaI <sub>3</sub>	A30WI <sub>3</sub>
A02SrI <sub>3</sub>	A06CaCl <sub>3</sub>	A09CdBr <sub>3</sub>	A12BaBr <sub>3</sub>	A15HfCl <sub>3</sub>	A19BaBr <sub>3</sub>	A22TiCl <sub>3</sub>	A25CdI <sub>3</sub>	A28CaBr <sub>3</sub>	A30ZrCl <sub>3</sub>
A02TmI <sub>3</sub>	A06HgI <sub>3</sub>	A09HgBr <sub>3</sub>	A12CaBr <sub>3</sub>	A15HgI <sub>3</sub>	A19EuCl <sub>3</sub>	A22TmBr <sub>3</sub>	A25HfCl <sub>3</sub>	A28HfBr <sub>3</sub>	A31CdI <sub>3</sub>
A03EuCl <sub>3</sub>	A06MnCl <sub>3</sub>	A09TaCl <sub>3</sub>	A12HfI <sub>3</sub>	A15MgF <sub>3</sub>	A19RhCl <sub>3</sub>	A22WBr <sub>3</sub>	A25PbCl <sub>3</sub>	A28NbCl <sub>3</sub>	A31PdB <sub>3</sub>
A03PdB <sub>3</sub>	A06PbCl <sub>3</sub>	A09TiCl <sub>3</sub>	A12InBr <sub>3</sub>	A15TaBr <sub>3</sub>	A19TmCl <sub>3</sub>	A22YBr <sub>3</sub>	A25SmCl <sub>3</sub>	A28PdCl <sub>3</sub>	A31TmBr <sub>3</sub>
A03ScI <sub>3</sub>	A06PbI <sub>3</sub>	A09YbI <sub>3</sub>	A12SnCl <sub>3</sub>	A15TmI <sub>3</sub>	A19TmI <sub>3</sub>	A23CaI <sub>3</sub>	A25TII <sub>3</sub>	A28PtCl <sub>3</sub>	A31WI <sub>3</sub>
A03SnBr <sub>3</sub>	A06ScBr <sub>3</sub>	A09YI <sub>3</sub>	A13BiBr <sub>3</sub>	A15ZnF <sub>3</sub>	A19YI <sub>3</sub>	A23CdBr <sub>3</sub>	A25TmI <sub>3</sub>	A28SnI <sub>3</sub>	A31YBr <sub>3</sub>
A03SnI <sub>3</sub>	A06SmBr <sub>3</sub>	A10PbCl <sub>3</sub>	A13HgI <sub>3</sub>	A16BiI <sub>3</sub>	A20CaI <sub>3</sub>	A23CoCl <sub>3</sub>	A25YI <sub>3</sub>	A28TaBr <sub>3</sub>	A32CaBr <sub>3</sub>
A03SrCl <sub>3</sub>	A06WI <sub>3</sub>	A10SbI <sub>3</sub>	A13RhCl <sub>3</sub>	A16CaBr <sub>3</sub>	A20PbCl <sub>3</sub>	A23HgBr <sub>3</sub>	A26AuBr <sub>3</sub>	A28YbI <sub>3</sub>	A32EuI <sub>3</sub>
A03SrI <sub>3</sub>	A07BiI <sub>3</sub>	A10TiBr <sub>3</sub>	A13ScBr <sub>3</sub>	A16CdBr <sub>3</sub>	A20PtCl <sub>3</sub>	A23SbBr <sub>3</sub>	A26CuCl <sub>3</sub>	A28YBr <sub>3</sub>	A32MoCl <sub>3</sub>
A03WBr <sub>3</sub>	A07CaCl <sub>3</sub>	A10TII <sub>3</sub>	A13SnBr <sub>3</sub>	A16EuBr <sub>3</sub>	A20SbCl <sub>3</sub>	A23SbI <sub>3</sub>	A26PtCl <sub>3</sub>	A29HgBr <sub>3</sub>	A32ReCl <sub>3</sub>
A04AgBr <sub>3</sub>	A07InI <sub>3</sub>	A10TmI <sub>3</sub>	A13SrCl <sub>3</sub>	A16MnF <sub>3</sub>	A20ScI <sub>3</sub>	A23TII <sub>3</sub>	A26ReCl <sub>3</sub>	A29MnBr <sub>3</sub>	A32SrI <sub>3</sub>

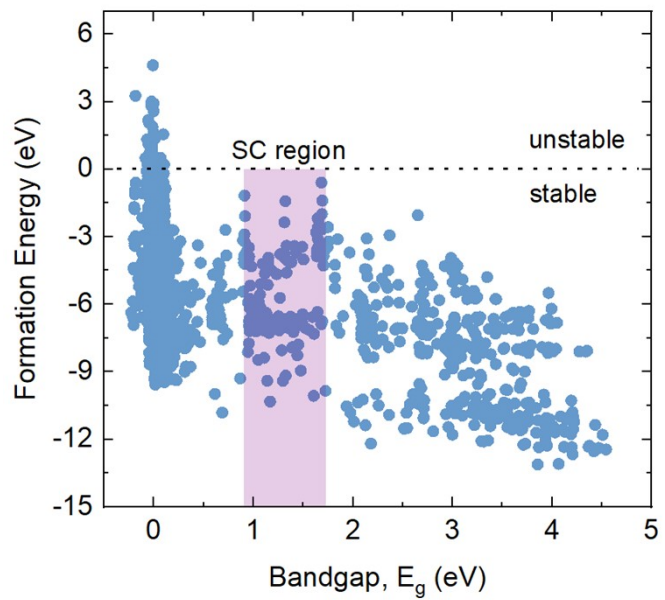


**Figure S7.** ML calculated crystal formation energy vs. bandgap plot of all hybrid perovskite candidates considered in this study. SC: semiconductor.

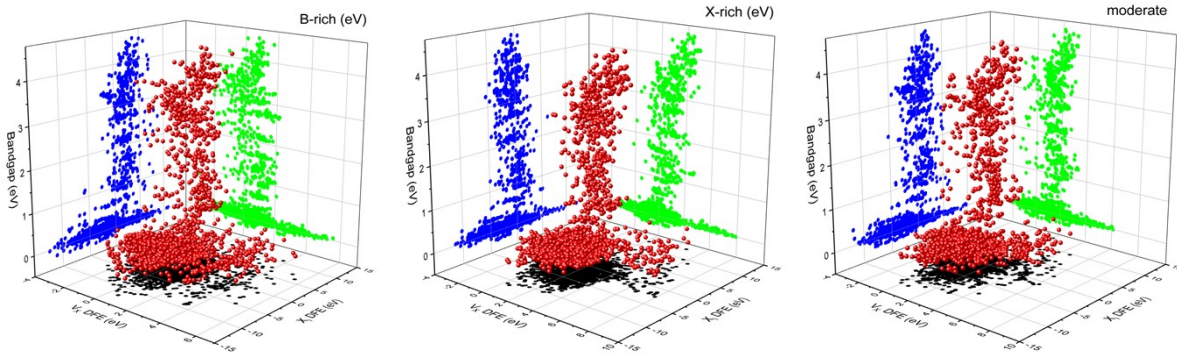


**Figure S8.** ML calculated 3D DFE vs. Bandgap plots for three different growth conditions. DFE: Defect formation energy.

**Table S7.** List of 190 promising defect-tolerant HOIP semiconductor candidates. Energies are in eV units.  $E_g$ : bandgap, DFE: Defect formation energy,  $\Delta H$ : crystal formation energy.

A	B	X	$E_g$	V <sub>X</sub> DFE			X <sub>i</sub> DFE			V <sub>X</sub>	X <sub>i</sub>	$\Delta H$
				B-rich	X-rich	mod.	B-rich	X-rich	mod.			
A01	Ca	Cl	3.31	-0.93	2.14	-0.27	1.19	-2.66	-1.65	4.39	-0.76	-10.63
A01	Hg	Cl	0.65	1.33	2.01	1.35	0.63	-1.08	-1.11	2.07	-0.36	-5.57
A01	Pb	Br	2.11	1.33	3.48	2.25	1.85	-0.60	-0.06	2.79	0.07	-6.96
A01	Pb	I	1.67	1.41	2.37	1.68	2.15	0.84	1.08	1.99	0.06	-3.53
A01	Sn	Br	0.99	1.43	3.42	2.43	1.08	0.34	0.33	1.54	0.03	-6.40
A01	Sn	Cl	1.09	1.95	3.28	2.43	1.07	0.52	-0.10	1.56	0.01	-6.50
A01	Zn	F	0.74	2.08	2.47	1.59	2.10	1.77	0.71	2.84	-0.55	-7.30
A01	Sn	I	0.94	1.34	2.17	1.78	1.59	0.84	1.20	1.44	0.10	-5.57
A02	Hg	Cl	0.66	1.48	1.93	1.53	1.03	-0.65	-0.80	2.48	-0.31	-3.93
A02	Sn	I	1.15	1.52	2.30	1.62	2.04	0.80	1.56	1.39	0.09	-3.87
A03	Pb	I	1.70	1.05	1.79	0.97	2.53	0.44	1.42	1.95	0.05	-10.70
A04	Ca	Br	3.37	-1.44	2.25	0.65	0.89	-3.25	-1.62	4.34	-0.09	-10.11
A04	Ca	Cl	3.12	-1.64	1.35	-0.58	0.73	-4.63	-2.33	4.34	-0.45	-4.74
A04	Hg	Cl	0.63	1.28	1.75	1.25	-0.17	-2.24	-2.02	2.04	-0.34	-6.50

A04	Pb	Br	2.09	0.17	2.89	1.94	-0.31	-3.38	-2.24	2.68	0.06	-2.86
A04	Pb	I	1.64	0.25	1.87	1.37	0.21	-1.93	-0.36	1.88	0.07	-6.16
A04	Sn	Br	0.96	0.17	2.95	1.98	-0.55	-2.53	-1.71	1.48	0.03	-6.10
A04	Sn	Cl	1.07	0.61	2.82	1.98	-0.56	-2.54	-2.14	1.51	0.02	-3.21
A04	Sn	I	0.91	0.07	2.27	1.45	0.49	-1.96	-0.53	1.38	0.01	-1.06
A05	Ca	Br	3.32	-0.57	3.26	0.80	1.65	-0.16	0.47	4.31	0.05	-1.47
A05	Ca	Cl	3.06	-0.87	2.22	-0.75	0.46	-1.48	-0.86	4.50	-0.32	-5.90
A05	Hg	Cl	0.64	0.82	1.64	1.27	-0.17	-0.64	-0.65	2.06	-0.34	-7.32
A05	Pb	Br	2.08	1.29	3.24	1.98	1.26	0.02	0.78	2.66	0.03	-7.14
A05	Pb	Cl	2.69	1.69	3.18	2.23	0.71	0.02	-0.10	2.90	0.09	-3.87
A05	Pb	I	1.64	1.30	2.15	1.49	2.03	0.82	1.75	1.92	0.07	-6.95
A05	Sn	Br	0.96	1.26	3.22	2.33	1.06	1.51	1.36	1.46	0.04	-6.84
A05	Sn	Cl	1.06	1.69	3.01	2.33	1.25	1.57	0.67	1.49	0.09	-4.17
A05	Sn	I	0.91	1.25	2.44	1.88	2.13	1.45	1.82	1.42	-0.03	-11.05
A05	Sr	Cl	3.42	0.40	3.82	1.41	1.72	-0.74	0.33	3.97	-0.37	-8.65
A05	Yb	Br	2.97	0.92	2.60	1.50	1.82	0.81	0.64	3.24	-0.03	-5.79
A06	Hg	Cl	0.65	0.49	1.47	1.16	0.68	-0.26	-0.01	2.46	-0.38	-4.12
A06	Sn	I	1.15	1.06	2.38	1.54	2.92	2.20	2.61	1.42	0.04	-3.78
A07	Sn	I	1.31	1.10	2.44	1.93	1.46	0.32	0.76	1.41	0.02	-10.92
A07	Yb	Cl	3.38	0.09	2.26	1.89	-1.89	-3.42	-3.64	4.28	-0.86	-10.33
A08	Ca	Br	2.36	-0.08	2.95	0.69	1.79	-1.55	-0.03	4.35	0.04	-3.46
A08	Ca	Cl	1.17	-0.27	1.83	-0.59	-0.22	-2.87	-1.38	4.54	-0.29	-6.94
A08	Pb	I	1.68	1.24	2.08	1.47	2.76	0.15	1.40	1.88	0.04	-3.86
A08	Sn	Br	0.98	1.23	3.03	2.16	1.54	-0.71	1.07	1.48	0.02	-11.38
A08	Sn	I	0.92	1.18	2.23	1.71	3.16	-0.53	1.67	1.38	0.03	-10.82
A08	Sr	Br	2.13	0.44	3.79	2.01	1.48	-2.16	0.85	3.91	0.03	-6.34
A08	Sr	Cl	0.69	0.46	2.98	1.33	2.12	-3.60	0.05	3.99	-0.32	-7.33
A08	Sr	I	1.64	0.43	2.58	1.52	2.71	-0.80	2.13	3.50	0.02	-3.81
A09	Pb	Br	2.12	1.19	2.88	1.89	0.39	-1.04	-0.57	2.68	0.02	-4.15
A09	Pb	I	1.67	1.14	1.86	1.40	1.79	0.23	0.92	1.89	0.04	-5.69
A09	Sn	I	0.91	1.11	2.10	1.64	1.80	0.04	0.81	1.39	-0.04	-3.74
A10	Hg	Cl	0.65	1.10	1.74	1.36	-0.70	-1.79	-1.43	2.48	-0.80	-3.93
A10	Pb	I	1.67	0.79	1.92	1.48	1.57	0.07	0.98	1.88	0.05	-10.46
A10	Sn	I	1.31	0.86	2.05	1.63	1.34	-0.08	1.12	1.41	0.03	-3.62
A10	Yb	Br	3.07	0.09	3.02	1.87	0.79	-2.19	-0.44	4.00	-0.29	-6.93
A11	Ca	Cl	3.32	-0.16	2.14	-0.31	-0.80	-3.21	-1.77	4.53	-0.31	-3.95
A11	Pb	I	1.72	1.27	2.01	1.63	2.16	0.61	1.04	1.94	0.06	-8.85
A11	Sn	Br	1.01	1.23	3.06	2.26	0.63	-0.25	0.48	1.48	0.06	-9.99
A11	Sn	I	0.95	1.18	2.21	1.81	2.29	0.37	1.59	1.44	0.00	-9.40
A11	Yb	Br	3.00	0.82	2.71	1.61	1.95	-0.46	0.68	3.26	-0.01	-4.71
A13	Ca	Br	2.23	-0.42	2.96	0.69	0.75	-2.75	-1.30	3.96	0.00	-6.28
A13	Ca	Cl	1.14	-0.90	1.82	-0.82	-1.11	-3.95	-2.32	4.18	-0.33	-2.80
A13	Hg	Cl	0.63	0.45	1.56	1.09	-3.88	-2.52	-3.74	2.16	-0.38	-3.16
A13	Pb	Br	2.08	1.36	3.19	1.92	-0.15	-1.75	-2.05	2.53	0.07	-10.54

A13	Pb	I	1.63	1.35	2.06	1.43	1.15	-0.71	-1.95	1.79	0.03	-6.89
A13	Sn	I	0.90	1.29	2.22	1.71	2.19	-0.22	-2.39	1.29	0.01	-10.46
A13	Sr	Br	1.94	0.07	3.80	2.01	-1.30	-3.02	-2.76	2.84	0.03	-7.26
A13	Sr	I	1.68	0.06	2.83	1.52	-0.07	-1.65	-2.25	2.49	0.02	-3.62
A13	Sr	Cl	0.61	-0.66	3.22	0.97	-2.08	-4.47	-3.91	2.61	-0.06	-7.02
A14	Ca	Cl	3.33	-0.34	2.14	-0.31	-1.14	-3.35	-2.31	4.53	-0.31	-4.04
A14	Pb	Br	2.15	1.07	3.16	2.13	0.77	-1.11	-0.50	2.68	0.04	-10.91
A14	Pb	I	1.70	1.09	1.92	1.63	2.18	0.38	0.97	1.94	0.06	-10.51
A14	Sn	Br	0.99	1.04	3.06	2.26	0.21	-0.62	0.19	1.48	0.06	-6.84
A14	Sn	I	0.94	0.99	2.13	1.81	2.09	0.00	1.52	1.44	0.00	-6.53
A14	Yb	Cl	3.35	1.05	3.38	1.80	-1.81	-3.58	-2.39	3.57	-0.86	-5.12
A15	Ca	Br	3.23	-1.81	1.92	0.04	1.44	-1.20	-1.16	4.39	-0.83	-8.47
A15	Ca	Cl	2.99	-2.04	1.20	-1.06	1.28	-2.59	-1.50	4.42	-1.15	-7.24
A15	Ca	I	3.14	-1.41	0.67	-0.04	-0.60	0.57	0.05	3.07	-0.66	-7.31
A15	Ge	F	0.67	1.02	1.87	0.58	0.89	4.61	0.20	4.05	-1.42	-10.51
A15	Hg	Cl	0.68	1.10	1.75	0.50	0.00	-2.13	-1.06	2.16	-0.33	-5.47
A15	Ti	F	1.05	-0.75	3.67	1.55	-0.08	-1.63	-0.61	3.71	-1.16	-7.06
A15	Yb	Br	2.99	0.02	2.50	1.21	0.44	-1.71	-1.15	3.26	-0.02	-6.88
A15	Yb	Cl	3.23	0.43	2.80	1.44	-0.60	-3.28	-2.31	3.41	-0.33	-3.55
A15	Mg	F	0.87	-3.09	0.54	-0.89	5.54	1.94	3.75	7.79	-4.23	-6.65
A15	Zn	F	1.86	-0.35	2.07	0.66	5.01	2.34	3.71	4.23	-1.65	-6.54
A16	Ca	Cl	3.21	-1.18	1.79	-0.39	1.26	-2.66	-0.81	4.34	-0.92	-3.83
A16	Hg	Cl	0.63	1.30	2.02	1.26	0.70	-1.38	-0.71	2.04	-0.36	-11.46
A16	Pb	Br	2.09	1.30	3.27	2.12	1.92	-0.60	0.32	2.74	0.06	-6.63
A16	Pb	Cl	2.70	2.03	3.24	2.37	1.44	-0.49	0.07	2.97	0.09	-6.36
A16	Pb	I	1.64	1.38	2.21	1.55	2.22	0.84	1.52	2.00	0.05	-2.66
A16	Sn	Br	0.96	1.30	3.33	2.06	1.24	0.34	0.87	1.48	0.03	-3.40
A16	Sn	Cl	1.07	1.82	3.20	2.06	1.23	0.52	0.75	1.51	0.01	-11.02
A16	Sn	I	0.91	1.20	2.61	1.53	1.80	0.92	1.72	1.44	-0.01	-10.37
A16	Ca	Br	3.46	-0.87	2.69	0.83	1.44	-1.52	-0.11	4.34	-0.68	-7.13
A16	Yb	I	3.02	1.19	2.99	1.81	2.29	0.20	1.62	3.23	-0.02	-10.88
A17	Ba	Br	2.96	0.26	2.91	2.08	3.15	-0.78	2.87	4.74	0.06	-5.06
A17	Pb	Br	2.15	1.15	2.42	1.67	1.95	-1.24	0.83	3.01	-0.06	-6.21
A17	Pb	Cl	2.80	1.31	2.23	1.59	1.09	-1.03	-0.06	3.41	-0.07	-10.12
A17	Pb	I	1.69	1.13	1.42	1.10	3.07	1.20	2.81	2.14	0.02	-10.83
A17	Sn	I	1.33	1.13	2.26	1.51	3.47	1.16	2.09	1.29	0.01	-10.24
A17	Sr	Br	2.71	-0.27	2.95	1.52	2.47	2.48	0.89	3.82	-0.01	-5.59
A17	Sr	Cl	2.05	-0.33	2.42	1.21	1.44	1.49	-0.05	4.07	-0.84	-7.09
A17	Sr	I	2.43	-0.30	1.95	0.96	3.34	6.24	3.09	3.65	-0.03	-3.65
A18	Ba	Br	2.93	-0.89	1.19	1.28	3.03	-1.10	1.68	3.87	-0.10	-3.98
A18	Ba	I	2.68	-1.10	1.04	0.83	3.46	0.25	2.24	4.21	-0.17	-11.37
A18	Pb	Br	2.13	0.38	0.98	0.94	1.21	-1.33	-0.72	2.99	-0.45	-10.82
A18	Sr	Br	2.67	-0.68	1.23	0.23	1.27	-1.93	-0.89	3.14	-0.52	-8.15
A19	Ca	Br	3.19	-0.70	3.09	0.83	1.83	-1.53	0.31	4.02	0.01	-10.43

A19	Ca	Cl	2.10	-0.91	1.97	-0.72	1.44	-2.84	-1.02	4.42	-0.30	-9.84
A19	Hg	Cl	0.65	1.13	2.04	1.47	0.74	-1.29	-1.24	2.29	-0.36	-6.78
A19	Pb	Br	2.09	1.56	3.35	2.12	1.78	-0.33	0.77	2.53	0.07	-3.11
A19	Pb	I	1.64	1.51	2.24	1.55	2.25	0.47	1.65	1.79	0.03	-3.49
A19	Sn	I	0.91	1.51	2.49	1.91	2.31	0.65	1.54	1.29	0.01	-10.62
A19	Sr	Br	3.22	0.86	4.50	2.37	2.88	-0.83	0.70	3.18	-0.02	-10.07
A19	Sr	Cl	1.98	0.72	4.22	1.67	1.90	-2.26	-0.80	2.96	-0.40	-10.55
A19	Yb	Br	2.67	0.75	2.74	1.71	2.21	-0.20	0.22	3.16	-0.08	-7.27
A20	Ca	Br	2.66	-0.91	2.56	0.22	1.86	-1.38	-0.06	4.13	0.04	-3.46
A20	Ca	Cl	1.72	-0.69	1.37	-1.17	0.47	-2.86	-1.74	4.42	-0.28	-6.64
A20	Pb	Br	2.09	0.56	2.86	1.42	2.22	0.14	1.10	2.53	0.08	-10.50
A20	Pb	I	1.65	0.55	1.63	0.92	2.65	0.92	2.05	1.79	0.03	-5.82
A20	Sn	I	0.96	0.49	1.65	1.16	3.06	0.73	2.90	1.29	0.02	-3.47
A20	Sr	Br	2.71	-0.16	3.21	1.58	3.34	-0.56	1.57	3.18	0.01	-3.78
A20	Sr	Cl	1.61	-0.47	2.42	0.80	3.98	-1.92	0.31	2.96	-0.18	-10.43
A20	Ca	I	2.35	-0.87	1.30	0.50	2.12	-0.28	0.90	2.61	-0.04	-7.74
A20	Sr	I	2.24	-0.36	1.85	1.09	3.33	0.57	2.64	2.83	0.10	-10.87
A21	Ca	Cl	3.35	-0.43	2.64	-0.28	0.99	-3.13	-1.96	4.73	-0.08	-6.17
A21	Pb	Cl	2.70	1.03	3.64	1.92	3.36	-0.27	-0.33	2.92	0.08	-6.55
A21	Pb	I	1.65	0.99	2.14	1.84	3.11	1.35	2.13	1.89	0.10	-7.52
A22	Ba	I	3.41	-0.04	2.55	2.10	4.05	0.13	2.89	3.78	0.07	-3.87
A22	Ca	Cl	2.26	-1.53	1.42	-0.86	-0.01	-3.66	-1.98	4.53	-0.35	-7.20
A22	Ca	I	2.87	-0.93	1.50	0.56	2.11	-0.88	0.63	2.88	0.06	-7.08
A22	Pb	I	1.74	0.78	1.08	1.13	2.76	0.41	1.55	1.89	0.05	-4.20
A22	Sn	I	1.27	0.92	1.89	1.42	3.55	0.18	2.51	1.43	0.04	-9.26
A22	Sr	Cl	2.57	-0.17	2.31	1.04	0.95	-3.44	-1.16	3.39	-0.75	-4.58
A22	Yb	Br	0.96	-0.38	1.85	1.32	1.97	-0.42	0.37	3.54	-0.10	-5.14
A22	Ca	Br	3.10	-2.00	2.64	0.22	1.18	-2.47	-0.79	4.37	-0.03	-6.12
A23	Ca	Cl	3.28	-0.05	2.42	-0.22	1.52	-0.74	-0.88	4.34	-0.28	-2.59
A23	Hg	Cl	0.65	1.24	2.01	1.62	1.05	-0.76	-0.65	2.04	-0.34	-5.17
A23	Mg	F	1.14	-0.49	1.48	0.50	2.03	0.43	1.02	7.56	-1.43	-5.11
A23	Pb	Br	2.09	1.15	3.39	2.28	2.32	0.17	0.44	2.68	0.08	-9.13
A23	Pb	I	1.64	1.22	2.29	1.71	2.74	1.44	1.64	1.88	0.08	-6.21
A23	Sn	Br	0.96	1.29	3.35	2.51	1.55	2.44	0.75	1.48	0.04	-4.19
A23	Sn	Cl	1.07	1.84	3.22	2.51	1.41	2.62	0.21	1.51	0.07	-5.75
A23	Sn	I	0.91	1.20	2.57	1.98	2.23	2.85	1.44	1.38	0.02	-2.18
A24	Ca	Cl	3.29	-0.93	2.27	-0.27	1.36	-0.42	-1.22	4.34	-0.28	-5.76
A24	Hg	Cl	0.65	1.31	2.01	1.35	0.94	-0.75	-0.69	2.04	-0.34	-5.57
A24	Mg	F	1.14	-1.35	1.39	0.46	1.73	0.58	1.89	7.56	-1.21	-2.90
A24	Pb	Br	2.09	1.33	3.39	2.25	2.00	0.48	0.36	2.68	0.08	-7.05
A24	Pb	I	1.65	1.41	2.29	1.68	2.31	1.75	1.51	1.88	0.08	-6.97
A24	Sn	Br	0.97	1.43	3.40	2.43	1.33	2.72	0.63	1.48	0.05	-9.54
A24	Sn	Cl	1.07	1.98	3.22	2.43	1.33	2.90	0.19	1.51	0.07	-8.95
A24	Yb	Br	3.00	1.20	3.71	2.08	1.25	-1.56	0.01	3.26	-0.29	-2.25

A25	Ca	Cl	3.28	-0.65	2.09	-0.27	1.42	-1.88	-1.09	4.60	-0.90	-2.70
A25	Ge	Cl	0.59	0.59	1.84	1.58	-1.27	1.33	0.06	0.98	-0.11	-9.73
A25	Hg	Cl	0.65	1.02	1.98	1.46	0.95	-0.01	-0.34	2.21	-0.67	-9.17
A25	Pb	Br	2.09	1.19	3.16	2.22	2.03	-0.07	0.86	2.79	0.00	-5.25
A25	Pb	I	1.65	1.20	2.09	1.65	2.08	0.26	1.82	1.97	0.05	-7.09
A25	Sn	Br	0.96	0.94	3.31	2.36	1.45	0.76	0.91	1.54	0.00	-6.50
A25	Sn	Cl	1.07	1.51	3.17	2.39	1.12	0.94	0.36	1.60	0.00	-4.45
A25	Sn	I	0.91	0.92	2.39	1.71	1.57	0.28	1.59	1.42	-0.05	-4.28
A25	Ti	F	1.26	-0.24	4.37	2.75	2.30	-0.99	2.70	2.57	-0.20	-0.60
A25	Yb	Br	3.03	0.82	2.65	1.66	2.04	-0.30	1.64	3.26	-0.34	-4.32
A26	Ca	Br	2.67	-0.63	2.82	0.48	4.27	-0.16	2.08	4.02	0.06	-1.17
A26	Ca	Cl	1.48	-0.60	1.70	-0.91	3.04	-1.61	0.78	4.42	-0.25	-6.50
A26	Pb	I	1.66	0.89	1.83	1.08	5.03	2.02	4.14	1.79	0.05	-11.52
A26	Sn	I	0.72	0.85	1.96	1.31	5.86	2.39	5.88	1.29	0.06	-11.64
A26	Sr	Br	2.69	0.21	3.66	1.84	6.19	0.58	3.72	3.18	0.00	-10.82
A26	Sr	Cl	1.33	0.19	2.87	1.05	6.99	-0.75	2.84	2.96	-0.21	-10.85
A26	Sr	I	2.21	0.16	2.31	1.34	6.12	1.72	4.79	2.83	0.06	-9.99
A27	Ca	Br	2.68	-1.08	2.53	0.04	4.12	0.64	1.26	3.46	0.00	-10.33
A27	Ca	Cl	1.49	-1.12	1.42	-1.35	2.56	-0.84	-0.11	3.73	-0.32	-8.15
A27	Pb	Br	2.13	0.49	2.50	1.14	4.35	1.81	2.47	2.57	0.05	-7.56
A27	Pb	Cl	2.69	0.89	2.19	1.19	4.59	1.44	1.59	2.81	0.07	-1.40
A27	Pb	I	1.68	0.45	1.32	1.08	5.18	3.50	3.48	1.83	0.00	-1.42
A27	Sn	Br	0.98	0.43	2.56	0.76	4.72	2.61	3.68	1.38	0.06	-8.70
A27	Sn	I	0.91	0.42	1.67	0.85	5.85	3.43	4.47	1.33	0.01	-8.14
A27	Sr	Cl	1.09	-0.37	2.26	0.08	7.75	0.02	1.67	1.67	-0.67	-5.15
A28	Ca	Cl	2.51	-1.84	1.56	-0.24	-0.14	-3.78	-1.70	4.67	0.06	-5.94
A28	Sr	Cl	2.81	-0.64	1.61	0.26	3.29	-3.55	0.26	3.15	-0.23	-11.50
A29	Ca	Cl	2.54	-1.32	2.31	0.20	-0.15	-3.15	-1.36	4.67	-0.11	-7.03
A29	Sr	Cl	3.03	-0.22	0.43	-0.01	3.60	-2.87	-0.72	3.74	0.09	-4.28
A29	Yb	Cl	3.23	0.10	3.32	1.70	-0.94	-3.01	-2.11	4.37	-0.81	-11.79
A30	Ca	Cl	2.60	-0.31	2.53	1.07	0.68	-2.83	-0.94	4.80	-0.08	-3.62
A30	Sr	Cl	3.10	0.50	2.33	1.83	5.07	-2.88	0.34	4.74	-0.03	-9.98
A31	Ca	Br	3.03	-1.57	2.65	0.24	3.26	-1.68	1.19	4.57	0.01	-10.34
A31	Ca	Cl	2.30	-1.37	1.42	-0.91	1.96	-3.04	0.24	4.73	-0.43	-9.98
A31	Pb	I	1.69	0.37	1.71	1.02	3.54	0.51	2.41	1.94	0.06	-10.08
A31	Sn	I	1.32	0.49	1.94	1.18	4.20	0.33	3.48	1.47	0.03	-9.30
A31	Sr	Br	3.01	-0.16	3.58	1.60	3.34	0.68	1.70	4.02	0.04	-7.27
A31	Sr	Cl	2.12	-0.06	3.02	1.06	2.76	-0.56	1.11	4.59	-0.26	-11.09
A31	Sr	I	2.79	-0.20	2.57	1.11	4.08	2.87	2.71	3.56	0.04	-6.57
A31	Yb	Br	2.47	0.24	1.99	1.21	3.36	0.44	2.47	3.53	-0.08	-5.27
A32	Ca	Cl	2.54	-1.73	1.88	-0.54	2.05	-2.42	-0.03	4.54	-0.11	-6.04
A32	Hg	Cl	0.69	0.50	1.56	0.81	3.59	0.99	-1.05	2.53	-0.37	-10.95
A32	Pb	I	1.70	0.01	1.23	0.99	4.10	2.76	2.15	1.97	0.07	-8.39
A32	Sr	Cl	3.00	-0.45	3.09	0.99	5.63	-1.46	1.49	3.43	0.02	-10.12

## References:

- [S1] W.-J. Yin, T. Shi, Y.-Y. Yan. Unusual defect physics in  $\text{CH}_3\text{NH}_3\text{PbI}_3$  perovskite solar cell absorber *Appl. Phys. Lett.*, 104, 063903 (2014).
- [S2] C. G. Van de Walle, J. Neugebauer. First-principles calculations for defects and impurities: Applications to III-nitrides *J. Appl. Phys.*, 95, 3851–3879 (2004).
- [S3] W. Ming, S. Chen, M.-H. Du. Chemical instability leads to unusual chemical-potential-independent defect formation and diffusion in perovskite solar cell material  $\text{CH}_3\text{NH}_3\text{PbI}_3$  *J. Mater. Chem. A*, 4, 16975–16981 (2016).
- [S4] T. Huang, S. Tan, S. Nuryyeva, I. Yavuz, F. Babbe, Y. Zhao, M. Abdelsamie, M. H. Weber, R. Wang, R.; K. N. Houk, C. M. Sutter-Fella, Y. Yang, Performance-Limiting Formation Dynamics in Mixed-Halide Perovskites. *Sci. Adv.* 7, eabj179 (2021).
- [S5] C. Freysoldt, J. Neugebauer, C. G. Van de Walle. Fully ab initio finite-size corrections for charged-defect supercell calculations. *Phys. Rev. Lett.*, 102, 016402 (2009).
- [S6] Y. Kumagai, F. Oba. Electrostatics-based finite-size corrections for first-principles point defect calculations. *Phys. Rev. B*, 89, 195205 (2014).
- [S7] C. Freysoldt, B. Grabowski, T. Hickel, J. Neugebauer, G. Kresse, A. Janotti, C. G. Van de Walle. First-principles calculations for point defects in solids. *Rev. Mod. Phys.*, 86, 253–305 (2014).
- [S8] Barca, G. M. J. et al. Recent developments in the general atomic and molecular electronic structure system. *J. Phys. Chem.* 152, 154102, (2020).
- [S9] M. H. Naik, M. Jain. CoFFEE: Corrections for formation energy and eigenvalues for charged defect simulations. *Comp. Phys. Comm.*, 226, 114-126 (2018).
- [S10] S. Lu, Q. Zhou, Y. Ouyang, Y. Guo, Q. Li, J. Wang. Accelerated discovery of stable lead-free hybrid organic-inorganic perovskites via machine learning. *Nat. Comm.* 9, 1–8 (2018).
- [S11] L., M. Mentel. Mendeleev - A python resource for properties of chemical elements, ions and isotopes, 2018.